Inorganic Chemistry

Article

pubs.acs.org/IC

Reactivity of Inorganic Sulfide Species toward a Heme Protein Model

Silvina A. Bieza,[†] Fernando Boubeta,[†] Alessandro Feis,[§] Giulietta Smulevich,[§] Darío A. Estrin,[†] Leonardo Boechi,*[,‡] and Sara E. Bari*[,†]

[†]Departamento de Química Inorgánica, Analítica y Química Física/INQUIMAE-CONICET, Facultad de Ciencias Exactas y Naturales, Universidad de Buenos Aires Ciudad Universitaria, Buenos Aires C1428EHA, Argentina

[‡]Instituto de Cálculo, Facultad de Ciencias Exactas y Naturales, Universidad de Buenos Aires Ciudad Universitaria, Buenos Aires C1428EHA, Argentina

[§]Dipartimento di Chimica "Ugo Schiff", Universita' di Firenze, Via della Lastruccia 3-13, 50019 Sesto Fiorentino, Firenze, Italy

Supporting Information

ABSTRACT: The reactivity of inorganic sulfide species toward heme peptides was explored under biorelevant conditions in order to unravel the molecular details of the reactivity of the endogenous hydrogen sulfide toward heme proteins. Unlike ferric porphyrinates, which are reduced by inorganic sulfide, some heme proteins can form stable Fe^{III}–sulfide adducts. To isolate the protein factors ruling the redox chemistry, we used as a system model, the undecapeptide microperoxidase (MP11), a heme peptide derived from cytochrome c proteolysis that retains the proximal histidine bound to the Fe^{III} atom. Upon addition of gaseous hydrogen sulfide (H_2S) at pH 6.8, the UV–vis spectra of MP11 closely resembled those of the low-spin ferric hydroxo complex (only attained at an alkaline pH) and cysteine or alkylthiol derivatives, suggesting that the Fe^{III} reduction was prevented. The low-frequency region of the resonance Raman spectrum revealed the presence of an Fe^{III}–S band at 366 cm^{-1} and the general features of a low-spin hexacoordinated heme. Anhydrous sodium sulfide (Na_2S) was the source of sulfide of choice for the kinetic evaluation of the process. Theoretical calculations showed no distal stabilization mechanisms for bound sulfide species in MP11, highlighting a key role of the proximal histidine for the stabilization of the Fe^{III}–S adducts of heme compounds devoid of distal counterparts, which is significant with regard to the biochemical reactivity of endogenous hydrogen sulfide.

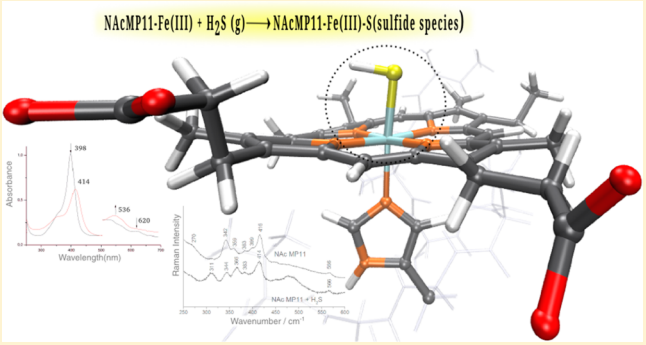

INTRODUCTION

Before the 1980s, when the endogenous production of hydrogen sulfide (H_2S) was assessed and described,[1−3] H_2S was only considered a toxic molecule.[4] The effect of H_2S in several physiological processes was derived from a considerable amount of research, revealing its role as signaling molecule in the cardiovascular system,[5] in pathologies such as Down syndrome or Alzheimer's disease,[6,7] in antioxidant activity,[8,9] or in the induction of hibernation states[10] as well as other important roles. The measurement of the steady-state levels of endogenous H_2S and related compounds is a current area of concern that is being actively reviewed,[11−15] with an impact on the characterization of its diverse physiological roles. H_2S is the third gasotransmitter to be discovered,[16,17] following nitric oxide (NO) and carbon monoxide (CO). For NO and CO, the term gasotransmitter seems unequivocal, whereas H_2S coexists with the anionic conjugate bases hydrosulfide, HS^-, and sulfide, S^{2-}.[18]

The miscellaneous biochemical roles of sulfide are a strong motivation for the studies of its chemical reactivity and potential biochemical targets. The recognized biochemical targets for sulfide are thiol compounds,[11,19] heme proteins,[20−22] and other metalloproteins.[23] Because it is a strong reducing agent, the reaction of sulfide with biologically relevant oxidants is linked to the prevention of their cytotoxicity.[24] In parallel, the basics of the manipulation of sulfide sources for the control of experimental conditions is being revisited because this has been proven critical to the evaluation of reactivity.[25−28] Gaseous H_2S has been regarded as the purest source of sulfide.[27] Upon dissolution in water at neutral pH (pK_{a1} = 6.98, 25 °C), the conjugated base HS^- forms and coexists with the dissolved gas at an almost equimolar concentration.[29] The autoxidation of these species must be considered in order to evaluate their reactivity: the air oxidation of H_2S is a slow process, whereas HS^- is easily oxidized, generating sulfur that can be further converted into soluble polysulfides (HS_n^-) in the presence of excess HS^-. This oxidation is evidenced in most commercial solid sources, such as $HSNa{\cdot}2H_2O$ or $Na_2S{\cdot}9H_2O$, as a yellowish layer in the material.[26] Anhydrous Na_2S is regarded

Received: September 20, 2014
Revised: December 3, 2014
Accepted: December 3, 2014
Published: December 24, 2014

DOI: 10.1021/ic502294z
Inorg. Chem. 2015, 54, 527−533

as a reliable source of solid sulfide because it is more resistant to autoxidation upon storage under inert atmosphere. Although the formation of oxidized sulfide species cannot be strictly avoided, the use of gaseous H_2S or anhydrous Na_2S keeps autoxidation to a minimum and improves the description of the isolated effect of sulfide.

One of the widely recognized biochemical targets for sulfide species is the heme moiety. The reported reactivity of H_2S toward heme compounds is diverse. It has been known for a long time that the reaction of excess H_2S toward metmyoglobin forms a green derivative, as a consequence of the formation of a sulfheme complex.[30−32] These compounds are considered diagnostic of H_2S deleterious effects,[33] but they have also been regarded as exerting a protection against H_2S toxicity.[34] Also, metal-centered reactions have been described for the reaction of inorganic sulfides with ferric porphyrinates. This type of reactivity has only been explored in organic media, with one case (later disputed) in which a low-spin ferric sulfide complex was inferred[35] and two other cases where ferrous sulfide complexes have been isolated and characterized.[36,37] In living organisms, porphyrinates exist buried in the protein matrix, where residues from the proximal and distal sides can modulate the reactivity of the heme group. In this context, some heme proteins have been found to be reduced by sulfides,[38,39] whereas others can prevent reduction and form remarkably stable Fe^{III}−S(sulfide) adducts;[20,40,41] the structural description of these ferric complexes is only speculative. Moreover, because heme reactivity within the protein matrix of heme proteins involves many variables that cannot be isolated, it is difficult to understand at the molecular level how this reactivity is controlled. Although the distal modulation of sulfide affinity has been actively studied, the influence of the proximal site is less appraised. In an attempt to fill this gap, we selected a minimalist model system devoid of distal amino acids. The microperoxidase 11 (MP11) is an undecapeptide derived from the proteolysis of cytochrome c that retains the two thioether linkages of the heme to Cys14 and Cys17 and to the proximal histidine (His18), providing an adequate model system for this purpose.[42,43] N-Acetyl derivatization (Fe^{III}NAcMP11, NAcMP11 = N-acetyl microperoxidase 11) prevents the aggregation of the heme peptide, which is undesired for ligand-binding studies.[44−46] The use of microperoxidases as representative models of heme proteins has been validated in several applications.[47−50] To meet the required experimental conditions for the evaluation of sulfide reactivity, we used gaseous H_2S and anhydrous Na_2S as sources of sulfide.

EXPERIMENTAL SECTION

Materials. All chemicals were of the highest purity available and were purchased from Sigma-Aldrich. Buffers were prepared with deionized water, containing DTPA (10^{-4} M). All experiments were performed using freshly prepared H_2S or anhydrous Na_2S (Sigma-Aldrich), which were stored in a glovebox under nitrogen (<1 ppm of O_2 and <1 ppm of H_2O). H_2S was prepared from $Na_2S{\cdot}9H_2O$ and phosphoric acid at room temperature, using Schlenk glass equipment under strict anaerobiosis. Solutions of Na_2S were prepared by the addition of argon-saturated phosphate buffers to the argon-purged solid material in containers with silicone septa and used within a day. In all of our cuvette studies, gastight Hamilton syringes were used to transfer the H_2S gas or the Na_2S solutions. The final concentration of sulfide was estimated using the absorbance of the sample at 230 nm (molar absorptivity = 7200 M^{-1} cm^{-1}).[27,28]

Theoretical Calculations. QM optimizations at PBE 6-31G** DFT level were performed on a ferric low-spin hexacoordinated-core porphyrinate, with both an imidazole ring and hydrosulfide (SH^-) as the fifth and sixth ligands, respectively. An *N*-methylacetamide molecule was used to provide a counterpart for hydrogen bonding to the imidazole ligand. A control calculation (full optimization at the same level of theory) was also performed in the absence of *N*-methylacetamide. Mülliken charge populations were computed for the optimized structures. Classical molecular dynamics (MD) simulations of $MP11Fe^{III}(HS^-)$ complex were performed with the Amber12 software package (Amberff-03). The structure of $MP11Fe^{III}$ was derived from the crystal structure of cytochrome c and conveniently truncated. Solvation was modeled by constructing a 9 Å cubic box using the TIP-3P model for water; 2 Na^+ ions were added for electro neutrality. Seven independent simulations (200 ns each) were performed to evaluate the system dynamics. To increase the configurational sampling space, accelerated molecular dynamics (aMD) simulations were performed. The aMD scheme modifies the classical potential energy by adding a bias potential ($\Delta V(r)$) that depends on a predefined threshold potential energy (E) and a tuning parameter (α) that determines how deeply the original potential energy will be modified, as shown in eqs 1 and 2:

$$V'(r) = \begin{cases} V(r), & V(r) \geq E \\ V(r) + \Delta V(r), & V(r) < E \end{cases} \quad (1)$$

$$\Delta V(r) = \frac{(E - V(r))^2}{\alpha + (E - V(r))} \quad (2)$$

where $V'(r)$ is the modified potential. The aMD approach is especially attractive because it does not require a priori knowledge of the reaction path.

Preparation of $NAcMP11Fe^{III}$−S(sulfide) Complex Using Gaseous H_2S. $NAcMP11Fe^{III}$−S(sulfide) complex was prepared according to published procedures,[46] using commercial $Fe^{III}MP11$ (Sigma-Aldrich) as the starting material. Solutions of $Fe^{III}NAcMP11$ (10^{-5}−10^{-6} M, buffer PO_4^{3-}, pH 6.8) were used for the absorbance measurements. The solutions (2.5 mL) were deaerated under a stream of argon for 30 min in screw-capped quartz cuvettes (1 cm) with silicon septa. H_2S was prepared from Na_2S and phosphoric acid at room temperature using Schlenk glass equipment under strict anaerobiosis. The addition of gaseous H_2S to the deoxygenated heme peptide solutions was performed using gastight syringes. In a typical experiment, 100 μL of gaseous H_2S (pH 6.8, 1 atm, 25 °C) was added to the stirred solution of $Fe^{III}NAcMP11$ (2.5 mL, 25 °C). Electronic absorbance spectra were recorded on a Hewlett-Packard HP 8453 spectrophotometer.

Preparation of $NAcMP11Fe^{III}$−S(sulfide) Complex Using Anhydrous Na_2S. The solutions assayed with gaseous H_2S were also assayed with Na_2S solutions. In a typical experiment, aliquots of buffered Na_2S solutions (pH 6.8) were added to the stirred solution of $Fe^{III}NAcMP11$ (2.5 mL, 25 °C). Final mixtures with ratios of sulfide/heme peptides = 1:1 and 100:1 were assayed and monitored spectroscopically. Electronic absorbance spectra were recorded on a Hewlett-Packard HP 8453 spectrophotometer.

Kinetic Analysis. Kinetic data were obtained by recording time-resolved UV−vis spectra using a SFM-300 Bio-Logic stopped-flow module equipped with a J&M TIDAS high-speed diode array spectrometer with combined deuterium and tungsten lamps (200−1015 nm wavelength range). Solutions were delivered through anaerobic ports, using PTFE cannulas. The syringes were controlled by three separate drives and were electronically controlled for the variation of the ratio of the reagents. The thermostat of the stopped-flow instrument was set at 25 °C. The system was operated using Bio-Kine 4.50 software, which was also used for data analysis. At least four kinetic runs were recorded for each experimental condition, and the reported data correspond to the mean values and standard deviations. All kinetic measurements were carried out under pseudo-first-order conditions unless otherwise stated. The reactions were studied at an ionic strength of 0.5 M (buffer PO_4^{3-}, pH 6.8).

For the estimation of k_{on}, the solutions of Na_2S were prepared by addition of deoxygenated buffer to the solid material under argon

DOI: 10.1021/ic502294z
Inorg. Chem. 2015, 54, 527−533

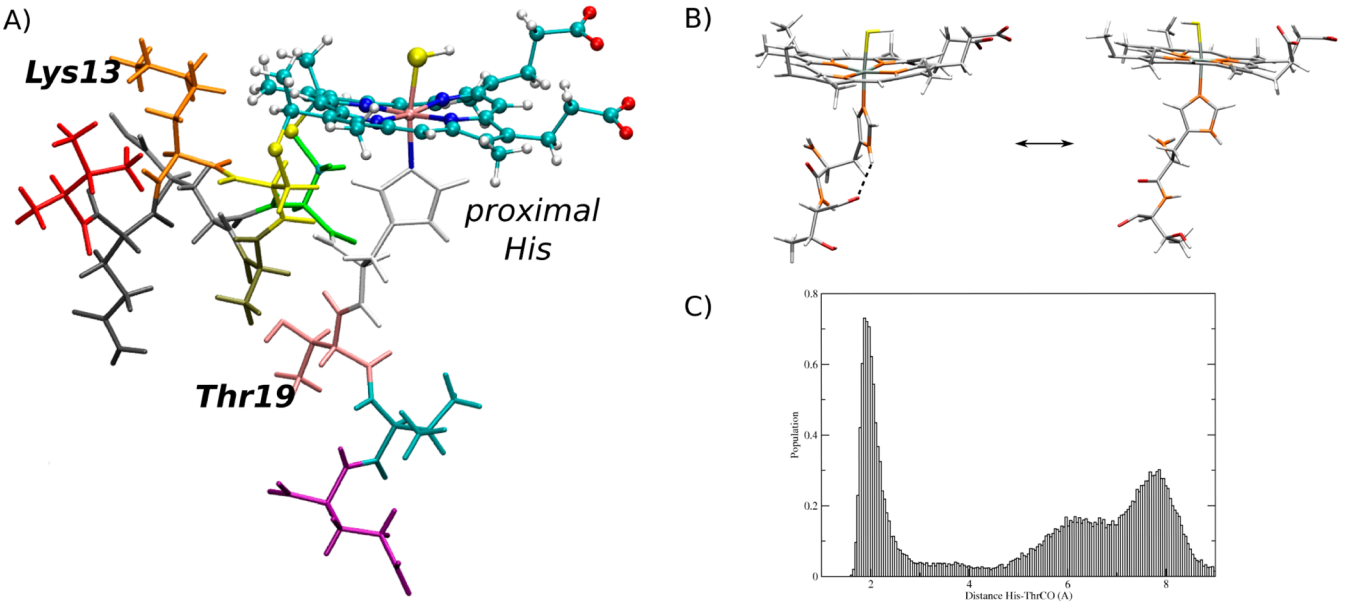

Figure 1. (A) Representative structure of Fe^{III}MP11 obtained from a snapshot of the MD simulations. (B) Dynamic hydrogen-bonding interaction between the N_δ of the proximal histidine and the carbonyl group of Thr19. The interaction induces a staggered conformation of the histidine with respect to the heme. (C) Histogram showing the distribution of distance N_δ(Im)−O(Thr19) along the MD trajectory, with the maximum centered around 2 Å (H bond).

atmosphere. The total observation time for each measurement was 0.4 s, and the dead time was 2 ms. The decrease of the 398 nm signal, characteristic of the Fe^{III}NAcMP11, was followed.

Kinetics of the release of the sulfide ligand from complex P_{414} ($[P_{414}] = 7 \times 10^{-6}$ M) were also studied using stopped-flow techniques under the general conditions described above, using 1-methylimidazol as the displacement reagent, with $[1\text{-MeIm}]/[P_{414}]$ varying from 100:1 to 1000:1. The total observation time for each measurement was 0.5 s, and the dead time was 4 ms. The formation of a new signal at 406 nm, with concomitant decrease of the signal at 414 nm, was followed. Data analysis is included in Figure S6.

Resonance Raman Spectroscopy. The resonance Raman (RR) spectra were recorded in a rotating 5 mm NMR tube by excitation with the 413.1 nm line of a Kr^+ laser (Innova 300 C, Coherent). The backscattered light from a slowly rotating NMR tube was collected and focused into a triple spectrometer (composed of two Acton Research SpectraPro 2300i monochromators working in subtractive mode and, in the final stage, a SpectraPro 2500i monochromator with a grating of 3600 grooves/mm) equipped with a liquid-nitrogen-cooled CCD detector (Roper Scientific, Princeton Instruments). The RR spectra were calibrated to an accuracy of 1 cm^{-1} for intense isolated bands, on the basis of indene and CCl_4 as standards. $[Fe^{III}\text{NAcMP11}] = 1.4 \times 10^{-5}$ M (buffer PO_4^{3-}, pH 6.8, 0.1M) was used for the RR spectra. Using a gastight syringe, 100 μL of NAcMP11Fe^{III}−S(sulfide) complex (prepared using gaseous H_2S) was transferred to the deaerated NMR tube.

RESULTS

To evaluate any possible distal- or proximal-side interactions, we performed MD simulations (7 × 200 ns) of Fe^{III}MP11 with coordinated HS^-. We simulated non-N-acetylated Fe^{III}MP11 to exaggerate the availability of positively charged residues that may interact with the ligand coordinated on the distal side of the heme. The HS^- species was selected because it is the most probable species coordinated to Fe^{III}MP11 at neutral pH. During the time scale of our simulations, no residues were observed to interact with the coordinated HS^-. We argue that no distal-side interaction exists for Fe^{III}MP11 and that this would be even less likely for Fe^{III}NAcMP11. It has been previously reported that Lys13 is able to reach the iron on the distal side. However, this configuration was manually induced, and only a short simulation (7 ns) was performed to probe the stability of the configuration.[51] To further validate our MD results, we performed aMD simulations,[52] and the same result was attained. A representative structure depicting the proximal-side interactions is shown in Figure 1A. The simulations also revealed a dynamic hydrogen-bonding interaction between the N_δ of the proximal histidine and the carbonyl group of the backbone of the Thr19 (Figure 1B,C). Interestingly, the proximal histidine−hydrogen bonding changes the charge distribution around the heme center, making the HS^- species slightly more negative (Figure S1). Although hydrogen bond formation induces a rotation of the proximal histidine, the imidazole ring maintains a staggered conformation with respect to the heme (Figure 1B). Overall, Fe^{III}MP11 provides a model for the evaluation of the binding of sulfide species in the absence of distal effects.

Figure 2 depicts the absorption spectra recorded after the addition of gaseous H_2S to a deoxygenated solution of Fe^{III}NAcMP11 (pH 6.8). Three bands with maxima at 414 nm (Soret band), 536 nm (Q_v band), and 568 nm (Q_0 band) are observed within the minute time scale. This final spectrum exhibits the regular features of a low-spin-state Fe^{III} complex. It also closely resembles that of the corresponding hydroxo complex, which is obtained only above pH 9 ($pK_a = 9.56$)[42] and is also comparable to the spectra obtained after the addition of alkylthiols or L-cysteine (Figure S2).[53,54] The sulfide complex characterized by the absorption maximum at 414 nm, P_{414}, remains stable for 2 h in the absence of oxygen. We did not observe the formation of sulfheme species in our experiments.

The addition of 1-methylimidazole to sulfide complex P_{414} at pH 6.8 showed the substitution reaction yielding a NAcMP11Fe^{III}−(1-methylimidazole) complex (Figure S3A). The addition of dithionite yielded reduced Fe^{II}NAcMP11 (Figure S3B). These reactivity tests further support the ferric nature of the sulfide complex of NAcMP11.

DOI: 10.1021/ic502294z
Inorg. Chem. 2015, 54, 527−533

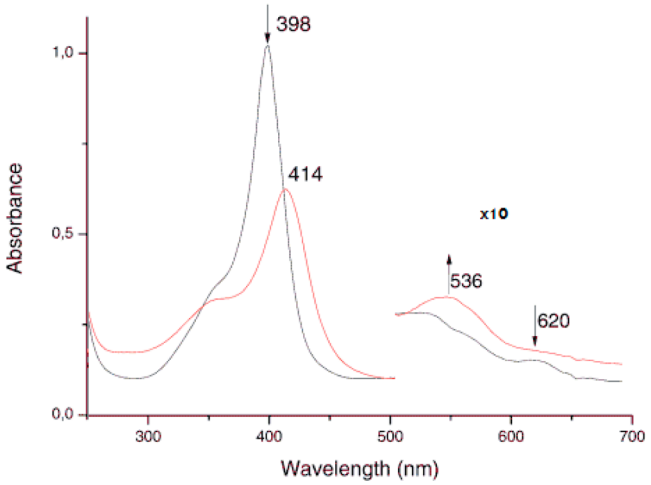

Figure 2. UV−vis spectra of Fe^{III}NAcMP11 in the absence or presence of H_2S (black or red, respectively), 30 min after the addition of the gas. [Fe^{III}NAcMP11] = 10^{-5} M, pH 6.8; gaseous H_2S (100 μL) was added to a 0.2 M buffered solution of PO_4^{3-} (2.5 mL).

RR spectroscopy was performed on sulfide complex P_{414} at pH 6.8 (Figure 3). A comparison with the spectra of the unbound form highlights the formation of a strong band at 366 cm^{-1}, an enhancement of the 311 cm^{-1} band, and a concomitant onset of a broad band centered at approximately 480 cm^{-1}. The latter is characteristic of a polymeric sulfur.[55] Compared with low-spin Fe^{III}−sulfide adducts, the 366 cm^{-1} band is tentatively assigned to the Fe−S stretching mode.[40,41] The rise of the band at 311 cm^{-1} can be explained as either an enhancement of the γ_7 and/or ν_{51} modes or a contribution from an Fe−SS stretching band (possibly caused by a disulfide formed in the reaction).[56,57] Neither of these bands was enhanced in the RR spectrum of the cysteine complex (Figure S4). No frequency change of the band at 383 cm^{-1}, assigned to a heme propionyl bending vibration, was observed after sulfide coordination, suggesting that no modification to the hydrogen bonding of the propionyl groups was achieved.[58]

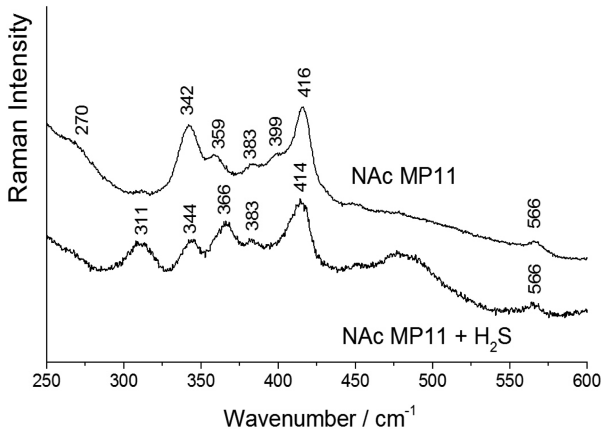

Figure 3. Low-frequency resonance Raman spectra of Fe^{III}NAcMP11 before and after the addition of gaseous H_2S at pH 6.8 (3 mW power, 1.2 cm^{-1} spectral resolution, 30 min integration time).

All of the above results are reproducible using gastight syringes for the administration of freshly prepared H_2S gas or deaerated buffered anhydrous Na_2S solutions. Similar results were also obtained using $NaHS{\cdot}H_2O$, but reproducibility was not ensured with this source of sulfide. The formation of the ferrous form was spuriously observed at pH 6.8 and was attributed to the formation of contaminants in the sulfide solutions.

Fe^{III}NAcMP8, the N-acetylated heme octapeptide from cytochrome c proteolysis, lacks the three amino acids of the N terminus of MP11 (including Lys13). Expectedly, reactivity toward inorganic sulfides similar to that of the undecapeptide analog was observed, confirming that the three N-terminal residues are not necessary for reactivity, which is also in agreement with our Fe^{III}MP11 simulation results.

The reaction of an equimolar sulfide/Fe^{III}NAcMP11 mixture was explored using anhydrous Na_2S. The reaction reached only partial conversion to a form with a broad Soret band (409−411 nm) after 60 min (Figure S5A). As observed with the addition of excess amounts of H_2S to the heme peptide, using an excess amount of anhydrous Na_2S ([sulfide]/[Fe^{III}NAcMP11]=100) led to the formation of P_{414} (Figure S5B).

Anhydrous Na_2S was used for stopped-flow kinetic studies. The reaction was performed under pseudo-first-order conditions (100:1 at pH 6.8) under strict anaerobiosis. Figure 4 depicts the time-resolved spectra showing the corresponding trace with maximum at 398 nm (Figure 4, inset) and the final complex (P_{414}). The analysis of the trace did not reveal sulfide concentration dependence for ratios of [sulfide]/[Fe^{III}NAcMP11] ranging from 100:1 to 400:1. To obtain information on the binding event, we explored lower ratios of [sulfide]/[Fe^{III}NAcMP11], outside of the range of pseudo-first-order conditions. The kinetic evolution data reveals a fast process that is linearly dependent on the concentration of sulfide during the onset of the reaction (Figure 5). The value of k_{on} ($(2.6 \pm 0.6) \times 10^4$ M^{-1} s^{-1}) represents an estimation on the binding constant. The linearity of this initial phase can be rationally assigned to the elementary binding step, $Fe^{III}NAcMP11 + H_2S \rightarrow NAcMP11Fe^{III}(SH_2)$ or $Fe^{III}NAcMP11 + SH^- \rightarrow NAcMP11Fe^{III}(SH^-)$.

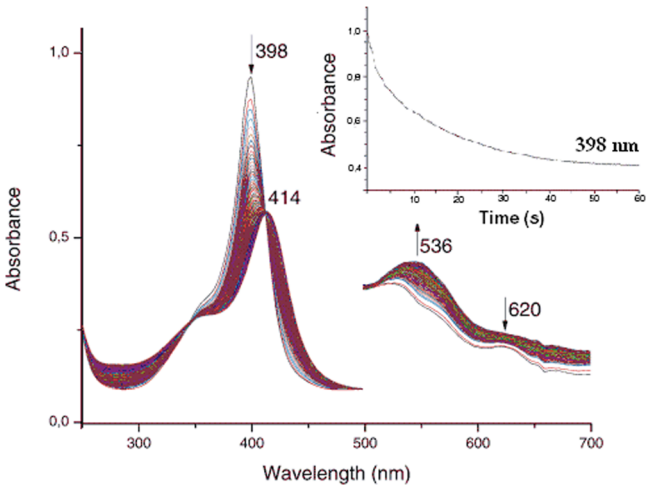

Figure 4. Rapid mixing of Fe^{III}NAcMP11 with different Na_2S concentrations (pseudo-first-order conditions, stopped-flow regime), leading to the final product, P_{414}. Inset: kinetic trace at 398 nm.

For the evaluation of the lability of the bound ligand, a ligand-displacement protocol was implemented with convenient concentrations of 1-methylimidazole and P_{414}. Figure 6 depicts the data derived using varying ratios of [1-MeIm]/[P_{414}], according to the kinetic analysis included in Figure S6.

DOI: 10.1021/ic502294z
Inorg. Chem. 2015, 54, 527−533

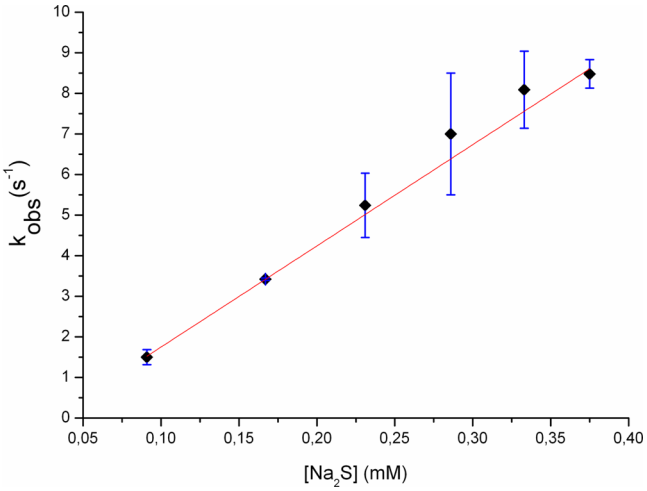

Figure 5. Rapid mixing of Fe^{III}NAcMP11 with increasing concentrations of Na_2S. Total observation time = 0.4 s, dead time = 2 ms, 25 °C. Concentration of [Na_2S] increased from 10^{-4} to 4×10^{-4} M. Each point represents a mean value of four independent measurements under a stopped-flow regime.

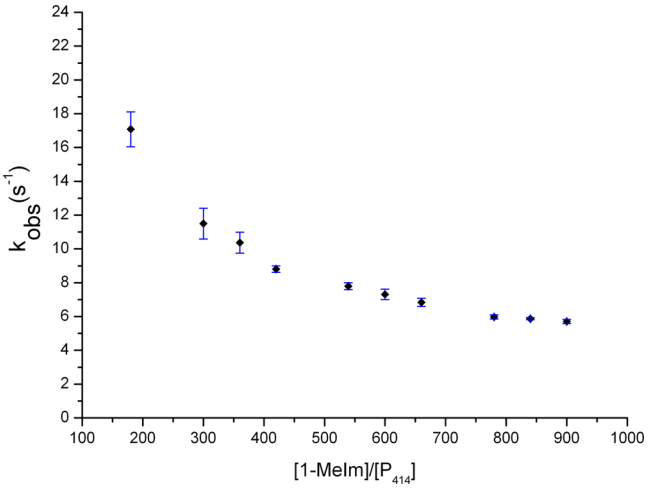

Figure 6. Rapid mixing of P_{414} with increasing concentrations of 1-methylimidazole (1-MeIm). Total observation time = 0.5 s, dead time = 4 ms, 25 °C. [1-MeIm]/[P_{414}] increased from 100:1 to 1000:1. Each point represents a mean value of four independent measurements under a stopped-flow regime.

The first-order rate constant thus obtained, $k_{off} = k_{obs} = (5.7 \pm 0.1)$ s^{-1}, is indicative of the stabilization provided solely by the histidine ligand.

DISCUSSION

The results obtained for the reaction at pH 6.8 of Fe^{III}NAcMP11 and excess inorganic sulfide, from either dissolved H_2S or anhydrous Na_2S, indicate the formation of a moderately stable reaction product, P_{414}, with a maximum absorbance at 414 nm that is stable for at least 2 h. In agreement with the absence of distal stabilization mechanisms, as assessed by computational experiments, the heme protein, excluding any interactions of the bound sulfide species with the environment other than those with the solvent. P_{414} exhibits spectroscopic features of a ferric low-spin species; the metal-centered reduction by inorganic sulfide was arrested devoid of any distal interactions. On the basis of our spectroscopic results, P_{414} can be tentatively assigned as the complex NAcMP11-Fe^{III}–(SH^-). The protonation state of the final reaction product remains to be confirmed. Our results are reproducible using either freshly prepared H_2S gas or anhydrous Na_2S as sources of inorganic sulfide, strongly pointing to the inherent (and different) reactivity of polysulfide contaminants usually present in other sources of sulfide.

The scenario is complicated by the inherent chemistry of sulfide species either bound or in solution, e.g., metal-catalyzed reactions, and the protonation states of the free and bound sulfide species. The absence of distal mechanisms of stabilization exposes the initially bound sulfide species to further reaction with, for example, excess sulfide.

A linearly dependent process is observed during the onset of the reaction; on the basis of an inspection outside of the pseudo-first-order conditions, this process was found to reasonably represent the binding of sulfide (H_2S or HS^-) to the ferric ion. The second-order rate constant derived from the kinetic analysis of the onset of the reaction is $(2.6 \pm 0.6) \times 10^4$ M^{-1} s^{-1}. This value is similar to those of the wild type truncated hemoglobins of *Bacillus subtilis* (Bs-trHb) and *Thermobifida fusca* (Tf-trHb), where a protein matrix interferes with free access to the ligand.[58] This result shows that the kinetic constant for Fe^{III}NAcMP11 is not enhanced by the absence of the protein environment but rather is controlled only by the surrounding water molecules. In fact, the kinetic binding constant for the triple mutant of Tf-trHb (WG8F, YCD1F, YB10F), which expels the water molecules of the distal cavity, is enhanced by 3 orders of magnitude.

The formation of the ferrous form upon treatment with dithionite of P_{414} was also observed for ferric sulfide complex HbI of *Lucina pectinata*,[40,41] whereas the ferric sulfide adducts of the truncated hemoglobins of *Bacillus subtilis* and *Thermobifida fusca* were inert. These considerations sketch the magnitude of the redox potential of the ferric sulfide complexes in the mentioned systems.

The value of the dissociation rate constant, $k_{off} = 5.7 \pm 0.1$ s^{-1}, represents an estimation of the isolated stabilizing effect of the sulfide ligand mediated by the proximal histidine residue. The value is in the upper range of the dissociation rate constants reported for the ferric sulfide complexes of certain hemoproteins.[58,59] In fact, the value is 1 order of magnitude higher than those of the triple and single mutants of Tf-trHb (WG8F, YCD1F, YB10F, $k_{off} = 2.2 \times 10^{-1}$ s^{-1} and WG8F, $k_{off} = 3.6 \times 10^{-1}$ s^{-1}, respectively); both mutants involve a critical distal tryptophan in the G8 region and exhibit the highest k_{off} values reported so far.[58,60] The dissociation rate constant has a value close to that reported for MP8Fe^{III}(CN^-).[61,62]

The stabilization of the ferric sulfide forms observed in a few heme proteins has been extensively attributed to a variety of distal-side sulfide interactions. For example, HbI from *Lucina pectinata* hemoglobin, which has an apolar cavity with three phenylalanines and a distal glutamine residue, shows very high sulfide stabilization.[40,41] However, Tf-trHb hemoglobin, which has a completely different structure, still displays a very high affinity for sulfide; this is due to the slow rate of sulfide release attained by a stabilization mechanism provided by a distal tryptophan residue. Moreover, among the three Hbs present in *Lucina pectinata* (I, II, and III), only HbI shows a very high sulfide affinity, and it has been proposed that the presence of TyrB10 in HbII and HbIII (PheB10 in HbI) destabilizes the binding of sulfide.[63] These results depict the complexity of the distal-side scenario that is under active discussion. As explained

DOI: 10.1021/ic502294z
Inorg. Chem. 2015, 54, 527–533

above, in the case of Fe^{III}NAcMP11, the environment provided by the water solvent does not severely impact the k_{on} value relative to that reported for sulfide-binding heme proteins, but the absence of distal stabilization interactions is responsible for the high value of k_{off}. As a consequence, the resulting affinity of Fe^{III}NAcMP11 for sulfide is at the lower limit of those in the currently reported data.

The reactivity of H_2S toward the heme c model compound reported herein, Fe^{III}NAcMP11, is different from that reported for the parent compound cytochrome c, which is reduced with equimolar amounts of NaHS, cysteine, gluthatione, or Na_2S.[25,38] These contrasting behaviors can be ascribed to different factors, such as the stabilization of reaction intermediates and products by distal residues or the accessibility of sulfide compounds or water molecules to the heme cavity and the ensuing differences in redox potentials. The difference between heme reduction potentials (E^0_{cytc} and $E^0_{NacMP11}$ = 263 and −134 mV, respectively; pH 7) has been attributed to the stabilization of the ferrous form by the distal methionine and the hydrophobicity of the cavity in native cytochrome c.[64] Accordingly, the replacement of the axial water molecule in Fe^{III}NAcMP11 by a N-acetyl methionine drives the reduction potential to a more positive value, that is, $E^0_{NAcMP11-AcMet}$ = −67 mV. A recent publication about the reactivity of cysteine toward engineered cytochrome c mutants and NAcMP8 highlights the versatile role of the protein environment in the speciation of the ligand and the redox stability of the heme.[65]

In summary, Fe^{III}NAcMP11 provides a model that is devoid of distal mechanisms of stabilization and kinetic barriers imposed by a protein structure, for the evaluation of proximal effects on the formation of a hexacoordinated complex with a sulfide species as the sixth ligand. The formation of a moderately stable, ferric low-spin species coordinated to a form of sulfide, characterized by a Soret maximum at 414 nm (P_{414}), is tentatively assigned to NAcMP11Fe^{III}(SH_2/SH^-) from the spectroscopic and kinetic data. These results suggest a key role of the proximal histidine in the binding of inorganic sulfide species to globins.

■ ASSOCIATED CONTENT

Supporting Information

Calculations at DFT/6-31G** level; representative structure from QM calculations and Mulliken charges; absorption spectra of the reactivity of the Fe^{III}−S(sulfide) complex toward 1-methylimidazole, azide, and dithionite; and absorption and resonance Raman spectra of the L-cysteine complex. This material is available free of charge via the Internet at http://pubs.acs.org.

■ AUTHOR INFORMATION

Corresponding Authors

*E-mail: lboechi@ic.fcen.uba.ar.
*E-mail: bari@qi.fcen.uba.ar.

Author Contributions

The manuscript was written through the contributions of all authors. S.A.B and F.B. contributed equally.

Notes

The authors declare no competing financial interests.

■ ACKNOWLEDGMENTS

S.A.B. and F.B. thank the Agencia Nacional de Promoción Científica y Tecnológica (ANPCyT) and Consejo Nacional de Investigaciones Científicas y Técnicas (CONICET), respectively, for their fellowships. D.A.E., L.B., and S.E.B. are CONICET staff. L.B. is the recipient of a Pew L.A. Fellowship. We thank Dr. José A. Olabe (University of Buenos Aires) for helpful discussions. We thank the University of Buenos Aires, ANPCyT, and CONICET for financial support. PICT-BID 2011-1266

■ REFERENCES

(1) Stipanuk, M. H.; Beck, P. W. *Biochem. J.* **1982**, *206*, 267−277.
(2) Abe, K.; Kimura, H. *J. Neurosci.* **1996**, *16*, 1066−1071.
(3) Hosoki, R.; Matsiki, N.; Kimura, H. *Biochem. Biophys. Res. Commun.* **1997**, *237*, 527−531.
(4) Beauchamp, R. O.; Bus, J. S.; Popp, J. A.; Boreiko, C. J.; Andjelkhovich, D. A. *Crit. Rev. Toxicol.* **1984**, *13*, 25−97.
(5) Polhemus, D. J.; Lefer, D. J. *Circ. Res.* **2014**, *114*, 730−737.
(6) Kamoun, P.; Belardinelli, M.; Chabli, A.; Lallouchi, K.; Chadefaux-Vekemans, B. *Am. J. Med. Genet., Part A* **2003**, *116*, 310−1.
(7) Ottani, A.; Zaffe, D.; Galantucci, M.; Strinati, F.; Lodi, R.; Guarini, S. *Neurobiol. Learn. Mem.* **2013**, *104*, 82−91.
(8) Filipovic, M. R.; Miljkovic, J.; Allgäuer, A.; Chaurio, R.; Shubina, T.; Herrmann, M.; Ivanovic-Burmazovic, I. *Biochem. J.* **2012**, *441*, 609−21.
(9) Lu, M.; Hu, L. F.; Hu, G.; Bian, J. S. *Free Radical Biol. Med.* **2008**, *45*, 1705−13.
(10) Collman, J. P.; Ghosh, S.; Dey, A.; Decréau, R. A. *Proc. Natl. Acad. Sci. U.S.A.* **2009**, *106*, 22090−22095.
(11) Ida, T.; Sawa, T.; Ihara, H.; Tsuchiya, Y.; Watanabe, Y.; Jamagai, Y.; Suematsu, M.; Motohashi, H.; Fujii, S.; Matsunaga, T.; Yamamoto, M.; Ono, K.; Devarie-Baez, N. O.; Xian, M.; Fukuto, J. M.; Akaike, T. *Proc. Natl. Acad. Sci. U.S.A.* **2014**, *111*, 7606−11.
(12) Wang, R. *FASEB J.* **2002**, *16*, 1793−98.
(13) Mani, S.; Cao, W.; Wu, L.; Wang, R. *Nitric Oxide* **2014**, *41*, 62−71.
(14) Kimura, H. *Nitric Oxide* **2014**, *41*, 4−10.
(15) Kolluru, G. K.; Shen, X.; Bir, S. C.; Kevil, C. G. *Nitric Oxide* **2013**, *35*, 5−20.
(16) Mustafa, A. K.; Gadalla, M. M.; Sen, N.; Kim, S.; Mu, W.; Gazi, S. K.; Barrow, R. K.; Yang, G.; Wang, R.; Snyder, S. H. *Sci. Signaling* **2009**, *2*, ra72.
(17) Wang, R. *Trends Biochem. Sci.* **2014**, *39*, 227−232.
(18) The term *sulfide* refers to the total sulfide content, i.e., the sum of H_2S, HS^-, and S^{2-}.
(19) Kimura, H. *Neurochem. Int.* **2013**, *63*, 492−497.
(20) Nguyen, B. D.; Zhao, X.; Vyas, K.; La Mar, G. N.; Lile, R. A.; Brucker, E. A.; Phillips, G. N., Jr.; Olson, J. S.; Wittenberg, J. B. *J. Biol. Chem.* **1998**, *273*, 9517−9526.
(21) Boffi, A.; Rizzi, M.; Monacelli, F.; Ascenzi, P. *Biochim. Biophys. Acta* **2000**, *1523*, 206−208.
(22) Brittain, T.; Yosaatmadja, Y.; Henty, K. *IUBMB Life* **2008**, *60*, 135−138.
(23) Nishimori, I.; Vullo, D.; Minakuchi, T.; Scozzafava, A.; Osman, S.; AlOthman, Z.; Capasso, C.; Supuran, C. T. *Bioorg. Med. Chem. Lett.* **2014**, *24*, 1127−1132.
(24) Li, Q.; Lancaster, J. R., Jr. *Nitric Oxide* **2013**, *35*, 21−34.
(25) Wedmann, R.; Bertlein, S.; Macinkovic, I.; Böltz, S.; Milikovic, J. L.; Muñoz, L. E.; Herrman, M.; Filipovic, M. R. *Nitric Oxide* **2014**, *41*, 85−96.
(26) Nagy, P.; Pálinkás, Z.; Nagy, A.; Budai, B.; Tóth, I.; Vasas, A. *Biochem. Biophys. Acta.* **2014**, *1840*, 876−91.
(27) Hughes, M. N.; Centelles, M. N.; Moore, K. P. *Free Radical Biol. Med.* **2009**, *47*, 1346−1353.
(28) Greiner, R.; Pálinkás, Z.; Bäsel, K.; Becher, D.; Antelmann, H.; Nagy, P.; Dick, T. P. *Antioxid. Redox Signaling* **2013**, *19*, 1749−1765.
(29) Sun, W.; Nesic, S.; Young, D.; Woollam, R. C. *Ind. Eng. Chem. Res.* **2008**, *47*, 1738−1742.
(30) Keilin, D. *Proc. R. Soc. London, Ser. B* **1933**, *133*, 393−404.

DOI: 10.1021/ic502294z
Inorg. Chem. 2015, 54, 527−533

(31) Libardi, S.; Pindstrup, H.; Cardoso, D. R.; Skibsted, L. H. *J. Agric. Food Chem.* **2013**, *61*, 2883−2888.
(32) Ríos-González, B. B.; Román-Morales, E. M.; Pietri, R.; López-Garriga, J. *J. Inorg. Biochem.* **2014**, *133*, 78−86.
(33) Park, C. M.; Nagel, R. L. *N. Engl. J. Med.* **1984**, *310*, 1579−1584.
(34) Szábo, C. *Nat. Rev. Drug Discovery* **2007**, *6*, 917−935.
(35) English, D. R.; Hendrickson, D. N.; Süslick, K. S.; Eigenbrot, C. W., Jr.; Scheidt, W. R. *J. Am. Chem. Soc.* **1984**, *106*, 7258−7259.
(36) Balch, A. L.; Cornman, C. R.; Safari, N. *Organometallics* **1990**, *9*, 2420−2421.
(37) Pavlik, J. W.; Noll, B. C.; Oliver, A. G.; Schulz, C. E.; Scheidt, W. R. *Inorg. Chem.* **2010**, *49*, 1017−1026.
(38) Hill, B. C.; Nicholls, P. *Can. J. Biochem.* **1980**, *58*, 499−503.
(39) Nicoletti, F. P.; Thompson, M. K.; Franzen, S.; Smulevich, G. *J. Biol. Inorg. Chem.* **2011**, *16*, 611−619.
(40) Kraus, D. W.; Wittenberg, J. B. *JBIC, J. Biol. Chem.* **1990**, *265*, 6043−6053.
(41) Pietri, R.; Lewis, A.; León, R.; Casabona, G.; Kiger, L.; Yeh, S. R.; Fernández-Alberti, S.; Marden, M. C.; Cadilla, C. L.; López-Garriga, J. *Biochemistry* **2009**, *48*, 4881−4894.
(42) Marques, H. M. *Dalton Trans.* **2007**, 4371−4385.
(43) Munro, O. Q.; Marques, H. M. *Inorg.Chem.* **1996**, *35*, 3752−3767.
(44) Low, D. W.; Winkler, J. R.; Gray, H. B. *J. Am. Chem. Soc.* **1996**, *118*, 117−120.
(45) Laberge, M.; Vregdenhil, A. J.; Vanderkooi, J. M.; Butler, I.S. J. *J. Biomol. Struct. Dyn.* **1998**, *15*, 1039−1050.
(46) Carraway, A. D.; McCollum, M. G.; Peterson, J. *Inorg. Chem.* **1996**, *35*, 6885−6891.
(47) Baldwin, D. A.; Marques, H. M.; Pratt, J. M. *J. Inorg. Biochem.* **1987**, *30*, 203−217.
(48) Sharma, V. S.; Schmidt, M. R.; Ranney, H. M. *J. Biol. Chem.* **1976**, *251*, 4267−4272.
(49) Cheek, J.; Low, D. W.; Gray, H. B.; Dawson, J. H. *Biochem. Biophys. Res. Commun.* **1998**, *253*, 195−198.
(50) Tezcan, F. A.; Winkler, J. R.; Gray, H. B. *J. Am. Chem. Soc.* **1998**, *120*, 13383−13388.
(51) Riposati, A.; Prieto, T.; Shida, C. S.; Nantes, I. L.; Nascimento, O. R. *J. Inorg. Biochem.* **2006**, *100*, 226−238.
(52) Hamelberg, D.; Mongan, J.; McCammon, J. A. *J. Chem. Phys.* **2004**, *120*, 11919−11929.
(53) Sadeque, A. J. M.; Shimizu, T.; Hatano, M. *Inorg. Chim. Acta* **1987**, *135*, 109−113.
(54) Marques, H. M.; Rousseau, A. *Inorg. Chim. Acta* **1996**, *248*, 115−119.
(55) Kalampounias, A. G.; Andrikopoulos, K. S.; Yannopoulos, S. N. *J. Chem. Phys.* **2003**, *118*, 8460−8467.
(56) Kimura, Y.; Mikami, Y.; Osumi, K.; Tsugane, M.; Oka, J.-I.; Kimura, H. *FASEB J.* **2013**, *27*, 2451−2457.
(57) Khan, S. A. K.; Hughes, R. W.; Reynolds, P. A. *Vib. Spectrosc.* **2011**, *56*, 241−244.
(58) Nicoletti, F. P.; Comandini, A.; Bonamore, A.; Boechi, L.; Boubeta, F. M.; Feis, A.; Smulevich, G.; Boffi, A. *Biochemistry* **2010**, *49*, 2269−2278.
(59) Ramos-Alvarez, C.; Yoo, B. K.; Pietri, R.; Lamarre, I.; Martin, J. L.; Lopez-Garriga, J.; Negrerie, M. *Biochemistry* **2013**, *52*, 7007−7021.
(60) Bonamore, A.; Ilari, A.; Giangiacomo, L.; Bellelli, A.; Morea, V.; Boffi, A. *FEBS J.* **2005**, *272*, 4189−201.
(61) Smith, M. C.; McLendon, G. *J. Am. Chem. Soc.* **1980**, *102*, 5666−5670.
(62) Marques, H. M.; Baldwin, D. A.; Pratt, J. M. *J. Inorg. Biochem.* **1987**, *29*, 77−91.
(63) Fernández-Alberti, S.; Bacelo, D. E.; Binning, R. C., Jr.; Echave, J.; Chergui, M.; López-Garriga, J. *Biophys. J.* **2006**, *91*, 1698−709.
(64) Battistuzzi, G.; Borsari, M.; Cowan, J. A.; Ranieri, A.; Sola, M. *J. Am. Chem. Soc.* **2002**, *124*, 5315−5324.
(65) Zhong, F.; Lisi, G. P.; Collins, D. P.; Dawson, J. H.; Pletneva, E. V. *Proc. Natl. Acad. Sci. U.S.A.* **2014**, *111*, E309−E315.

DOI: 10.1021/ic502294z
Inorg. Chem. 2015, 54, 527−533